Large-strain self-weight consolidation of dredged sludge

Hao Zhang[1]; Sijie Liu[2]; Honglei Sun[3]; Yuanqiang Cai[4]; Xueyu Geng[5]; Xiaodong Pan[6]; Yongfeng Deng[7]

Abstract: Prediction for self-weight consolidation of dredged sludge is important for its reuse in civil engineering applications. In this work, considering the special non-linear relationships of e-k and e-σ' for dredged sludge, Gibson's large strain consolidation equation was modified to simulate the self-weight consolidation process of dredged sludge. Using the finite difference method (FDM), the influences of four main parameters, including initial height, initial void ratio, void ratio at liquid limit and specific gravity of soil particles, on the consolidation process of dredged slurry were analyzed. For the above four parameters, the self-weight consolidation of dredged slurry is most sensitive to the variation of void ratio at liquid limit, while its response to the change of specific gravity of soil particles is relatively subtle. Consolidation behaviors under other commonly used constitutive models were also calculated for comparison. It was found that the total settlement obtained by the present relation is larger than the results obtained using typical nonlinear constitutive relations, and the speed of consolidation is higher.

Key words: large-strain; self-weight consolidation; dredged sludge; non-linear; constitutive relations

[1] Ph.D. Candidate, Research Center of Coastal and Urban Geotechnical Engineering, College of Civil Engineering and Architecture, Zhejiang University, Hangzhou 310058, China.
[3] Ph.D. Candidate, Research Center of Coastal and Urban Geotechnical Engineering, College of Civil Engineering and Architecture, Zhejiang University, Hangzhou 310058, China.
[2] Professor, College of Civil Engineering, Zhejiang University of Technology, Hangzhou 310000, China (Corresponding author). E-mail: sunhonglei@zju.edu.cn
[4] Professor, Research Center of Coastal and Urban Geotechnical Engineering, College of Civil Engineering and Architecture, Zhejiang University, Hangzhou 310058, China; and Professor, College of Civil Engineering, Zhejiang University of Technology, Hangzhou 310000, China.
[5] Associate professor, School of Engineering, University of Warwick, Coventry CV4 7AL, UK.
[6] Associate professor, College of Civil Engineering, Zhejiang University of Technology, Hangzhou 310000, China.
[7] Professor, Institute of Geotechnical Engineering, School of Transportation, Southeast University, Nanjing 210018, China.

Introduction

With the continuous progress of urbanization, a large volume of dredged sludge is produced by dredging rivers, ports and harbors, causing land occupation and environmental pollution problems (He et al. 2020; Lang et al. 2020a). In engineering applications, reusing treated dredged sludge as reclaimed soils, backfilling or building materials can solve the problems effectively (Wang et al. 2019; Lang et al. 2021). However, the dredged sludge typically contains high water content and rich organic matter, leading to its low strength and high compressibility (Du et al. 2019; Lang et al. 2020b, He et al. 2020; Wang et al. 2020). In engineering practice, before subsequent treatment on the dredged fills using vacuum pressure or other methods, self-weight consolidation is usually proceeded to form enough strength to withstand the instrument and equipment (Wang et al. 2020). Therefore, predicting the self-weight consolidation process of these slurries is important in deciding when the following improvement starts.

Several models have been developed to study the one-dimensional consolidation process, of which the most widely used ones are the infinitesimal strain model proposed by Terzaghi (1924) and the finite strain model introduced by Gibson et al. (1967; 1981). Terzaghi's (1924) one-dimensional small strain consolidation theory is based on some simplified assumptions, making the form simple but limiting the range of applications. Mikasa (1965) found that Terzaghi's small strain consolidation theory cannot depict the consolidation characteristics in a series of consolidation tests and attributed the inaccuracy to the ignorance of self-weight stress in Terzaghi's theory. Removing the small strain assumption and considering the self-weight, Gibson et al. (1981) established the large strain consolidation equations in the flow coordinate system with consideration of coordinate error caused

by the soil's excessive settlement, which is more realistic.

Constitutive relation is also crucial for the analysis of soil consolidation characteristics. Different constitutive models are based on different conditions, and may only be applicable to specific soil types (Schiffman et al. 1994). Lee and Sills (1981) used the linear $e-\sigma'$ relationship ($\sigma'=\alpha(e_0-e)$) and linear $e-k$ relationship ($k=\gamma_f k_0(e+1)$) in a soft fill's large-strain self-weight consolidation problem to obtain an analytical solution, which is convenient, but the linearization goes beyond the soil properties. To better describe the actual consolidation process, assuming the consolidation coefficient is constant, some people adopted the nonlinear variations of compressibility and permeability, in the forms of $m_v=-(\partial e/\partial\sigma')/(1+e)$ (Davis and Raymond 1965), $e-\log p$, $k_v=k_F(1+bu^n)$ (Barden and Berry 1965), $p/\varepsilon=E_0+np$ (Wei 1993), and some others (Mikasa 1965; Cargill 1984; Mcvay et al. 1987; Hawlader et al. 2008; Xie et al. 2009; Chai et al. 2014). However, the constant consolidation coefficient has a limited range of applications, and is basically reasonable for inorganic soils. For other soils, such as soft clay, the decreasing of consolidation coefficient in the consolidation process is not negligible (Poskitt 1969). Then, many models taking all the changes in compressibility, permeability and consolidation coefficient into account occurred, solving the consolidation problem in a more practical way (Fox and Berles 1997; Papanicolaou and Diplas 1999; Rujikiatkamjorn et al. 2007; Fox and Pu 2012; Pu et al. 2020). In the past decades of researches on soil's consolidation, the typical semi-logarithmic $e-\log\sigma'$, $e-\log k$ model (Talylor 1948; Mesri and Rokhsar 1974, Kessel and Kesteren 2002; Feng et al. 2019) and double-logarithmic $\log e-\log\sigma'$, $\log e-\log k$ model (Carrier 1984; Yao et al. 2002; Pu et al. 2020) were most widely accepted among these nonlinear consolidation models. However, their applicability in dredged slurries

has been questioned in recent years, due to the much higher water contents of dredged slurries than other soil types. Hong et al. (2010) and Cao et al. (2014) conducted a series of one-dimensional consolidation tests on different dredged sludges reconstituted at various initial water contents. They found that the relationships of $e-\sigma'$ and $e-k$ for clays with high initial water content, such as dredged sludge, were not the simple logarithmic types. The initial void ratio and void ratio at liquid limit play important roles in determining the relationships. However, these kinds of nonlinear compressibility and permeability models have not been considered in the self-weight consolidation of dredged sludge yet.

In this paper, a self-weight consolidation model was developed considering the special non-linear variations of permeability and compressibility for dredged sludge under large strain assumption. Gibson's one-dimensional large strain consolidation governing equation was discretized and solved by the finite difference method (FDM), in which the Crank-Nicolson difference format was chosen for its excellent stability and accuracy. Influences of four main parameters (initial height, initial void ratio, void ratio at liquid limit, and specific gravity of soil particles) on the consolidation process and the differences between various constitutive models in this model were further analyzed, to provide support for the settlement prediction in future projects.

Model description

The present constitutive model

Hong et al. (2010) conducted a series of tests on the soils with high water contents and summarized a special $e-\sigma'$ relationship, considering several parameters that are not commonly used

80 in the compression models. Different from the typical semi-logarithmic or double-logarithmic models
81 with only one smooth compression curve, the inverse 'S'-shaped compression curve in Hong et al.'s
82 (2010) model can be well represented by two straight lines in the bilogarithmic plot. The effective
83 vertical stress corresponding to the intersection point of the two straight lines in the bilogarithmic
84 graph is called suction pressure σ_s', which has a unique relationship with the normalized initial void
85 ratio relative to the void ratio at liquid limit e_0 / e_L (Hong et al., 2010). Meanwhile, intrinsic
86 compression index C_c^* and void ratio at the effective vertical stress of 100 kPa e_{100}^* are also
87 considered, both of which are affected by the initial water content and liquid limit (Hong et al., 2010).
88 These soil properties that are not involved in the traditional models make this model more distinctive.
89 Furthermore, based on Hong et al.'s (2010) work, an $e-k$ relationship and an extended $e-\sigma'$
90 relationship were proposed by Cao et al. (2014) in forms of Eqs. (1)-(2), and the expressions of $e-\sigma'$
91 differ under the conditions of $\sigma' < \sigma_s'$ and $\sigma' \geq \sigma_s'$. For a more accurate description, the
92 compression relation of dredged clays was partitioned into two parts with the remolded yield stress as
93 the dividing point. The diagrams of the permeability and compressibility models reported by Cao et al.
94 (2014) are shown in Fig. 1, units in cm/s and kPa.

95 $$k = 1.6\times10^{-7}\left(\frac{e}{e_L}\right)^{4.42} \tag{1}$$

96 $$e = \begin{cases} -0.06e_L^{-4.91}e_0^{2.77e_L^2-10.49e_L+13.3}\sigma' + e_0 & \sigma' < \sigma_s' \\ C_c^*\left[3.0 - 1.87\lg\sigma' + 0.179(\lg\sigma')^2\right] + e_{100}^* & \sigma' \geq \sigma_s' \end{cases} \tag{2}$$

97 where, e_L is the void ratio at liquid limit, e_{100}^* is void ratio of the reconstituted clays at the effective
98 vertical stress of 100 kPa, C_c^* is termed the intrinsic compression index, and σ_s' is the remolded
99 yield stress (i.e. suction pressure). These parameters can be estimated using the following empirical

100 equations when test results are not available (Hong et al. 2010).

101 $$e_{100}^{*} = 0.109 + 0.679e_L - 0.089e_L^2 + 0.016e_L^3 \tag{3}$$

102 $$C_c^{*} = 0.256e_L - 0.04 \tag{4}$$

103 $$\sigma_s' = 5.66 / (e_0 / e_L)^2 \tag{5}$$

104 ## *Governing equation*

105 Based on the flow coordinate system, the governing equation of large strain consolidation with

106 void ratio as the main variable in Gibson et al. (1981) is:

107 $$\pm\left(\frac{\gamma_s}{\gamma_f} - 1\right)\frac{\mathrm{d}}{\mathrm{d}e}\left[\frac{k(e)}{1+e}\right]\frac{\partial e}{\partial z} + \frac{\partial}{\partial z}\left[\frac{k(e)}{\gamma_f(1+e)}\frac{\mathrm{d}\sigma'}{\mathrm{d}e}\frac{\partial e}{\partial z}\right] + \frac{\partial e}{\partial t} = 0 \tag{6}$$

108 where, e is void ratio, k is the vertical permeability coefficient, γ_s and γ_f are the solid and

109 liquid gravity of the soil respectively, σ' is the effective stress, t is time, z is the time-

110 independent coordinate, and the relation between z and the actual position of soil plane a is

111 $dz / da = 1/(1+e_0)$. The reduced coordinate z was measured from the bottom plane, so the negative

112 sign in Eq. (6) must be taken.

113 For the convenience of calculation, Eq. (6) was transformed and simplified as:

114 $$\frac{\partial e}{\partial t} = A\frac{\partial^2 e}{\partial a^2} + B\left(\frac{\partial e}{\partial a}\right)^2 + C\frac{\partial e}{\partial a} \tag{7}$$

115 where,

116 $$A = -D\frac{\mathrm{d}\sigma'}{\mathrm{d}e} = \begin{cases} D\dfrac{1}{-0.06e_L^{-4.91}e_0^{2.77e_L^2-10.49e_L+13.3}} & \sigma' < \sigma_s' \\ D\left(\dfrac{10^{\frac{1.87-\sqrt{3.4969-0.716\left(3.0-\frac{e-e_{100}^{*}}{C_c^{*}}\right)}}{0.358}}\ln 10}{C_c^{*}\sqrt{3.4969-0.716\left(3.0-\dfrac{e-e_{100}^{*}}{C_c^{*}}\right)}}\right) & \sigma' \geq \sigma_s' \end{cases} \tag{8}$$

$$B = -\frac{\partial D}{\partial e}\frac{\mathrm{d}\sigma'}{\mathrm{d}e} - D\frac{\mathrm{d}^2\sigma'}{\mathrm{d}e^2} \tag{9}$$

$$C = -\frac{(\gamma_s - \gamma_f)}{\gamma_f}(1+e_0)\frac{\mathrm{d}}{\mathrm{d}e}\left[\frac{k}{1+e}\right] \tag{10}$$

$$D = \frac{k(1+e_0)^2}{\gamma_f(1+e)} \tag{11}$$

and, A, B, C, D, σ' and k are all functions of the void ratio e (Gibson et al. 1981).

Initial and boundary conditions

Assuming soils are homogeneous at the beginning of consolidation, the initial condition is:

$$e(a,0) = e_0, \quad 0 \le a \le a_0 \tag{12}$$

The upper boundary is considered as a free drainage boundary, so the boundary condition can be written as:

$$e(a_0,t) = e_0, \quad t \ge 0 \tag{13}$$

where, a_0 is the total thickness of the soil.

Supposing the bottom of the slurry is an undrained boundary, the change rate of the excess pore water pressure u with space coordinate a at the boundary is zero. That is:

$$\frac{\partial u}{\partial a}\Big|_{a=0} = \frac{\partial u}{\partial \xi}\frac{\partial \xi}{\partial a} = 0 \tag{14}$$

where, ξ is the convective coordinate changing with a and t. The relationship between ξ and a is (Gibson et al. 1981):

$$\frac{\partial \xi}{\partial a} = \frac{1+e}{1+e_0} \tag{15}$$

According to Peter and Smith (2002), the partial derivative of u to ξ is:

$$\frac{\partial u}{\partial \xi} = -\frac{\gamma_s - \gamma_f}{1+e} + \frac{1+e_0}{1+e}\frac{1}{a_v}\frac{\partial e}{\partial a} \tag{16}$$

The expression of the compression factor a_v is:

$$a_v = -\frac{\mathrm{d}e}{\mathrm{d}\sigma'} = \begin{cases} 0.06 e_L^{-4.91} e_0^{2.77 e_L^2 - 10.49 e_L + 13.3} & \sigma' < \sigma_s' \\ C_c^*\left(\dfrac{1.87 - 0.358 \lg \sigma'}{\sigma' \ln 10}\right) & \sigma' \geq \sigma_s' \end{cases} \tag{17}$$

Substituting Eqs. (15)-(17) into Eq. (14), the undrained boundary condition is:

$$\left.\frac{\partial e}{\partial a}\right|_{a=0} = \frac{\gamma_s - \gamma_f}{(1+e_0)} a_v \tag{18}$$

Finite difference solution

Many numerical methods, such as FDM, FEM, DQM, are convenient to solve the partial differential equations (Alimirzaei et al. 2019; Al-Furjan et al. 2020a, 2020b, 2020c, 2020d, 2020e; Hirian et al. 2021). In this paper, the FDM was adopted, which is often used in the consolidation problems. In the FDM, the soil is divided into I sublayers with a thickness of Δa for each sublayer, and the vertical distance from any sublayer's upper surface to the datum plane is $a = i\Delta a$. Time is divided into J small time periods Δt, and the time corresponding to the end of any time period is $t = j\Delta t$ [Fig. 2]. Ekolin (1991) proved the convergence and stability of the Crank-Nicolson difference scheme, when the mesh parameters (I, J) are greater than 65. For every case in this paper, Δa is 0.1 m, Δt is 0.001 a (i.e. year). Thus, the values of I and J in each group are all much larger than the recommended value. The correctness is guaranteed.

Crank-Nicolson type difference scheme is used to discretize Eq. (7) as:

$$\frac{e_i^j - e_i^{j-1}}{\Delta t} = A_i^{j-1}\frac{e_{i+1}^{j-1} - e_{i-1}^{j-1}}{2\Delta a} + \frac{1}{2}C_i^{j-1}\left(\frac{e_{i+1}^j + e_{i-1}^j - 2e_i^j}{\Delta a^2} + \frac{e_{i+1}^{j-1} + e_{i-1}^{j-1} - 2e_i^{j-1}}{\Delta a^2}\right) + B_i^{j-1}\left(\frac{e_{i+1}^{j-1} - e_{i-1}^{j-1}}{2\Delta a}\right)^2, \quad i = 1, 2, ..., I \quad j = 1, 2, ..., J \tag{19}$$

Classifying Eq. (19) by time nodes, the transformation below is available:

$$e_{i+1}^j - 2\left[1 + \frac{\Delta a^2}{\Delta t C_i^{j-1}}\right]e_i^j + e_{i-1}^j = -e_{i+1}^{j-1} + 2\left[1 - \frac{\Delta a^2}{\Delta t C_i^{j-1}}\right]e_i^{j-1} - e_{i-1}^{j-1} - \frac{A_i^{j-1}}{C_i^{j-1}}\Delta a(e_{i+1}^{j-1} - e_{i-1}^{j-1}) - \frac{B_i^{j-1}}{2C_i^{j-1}}(e_{i+1}^{j-1} - e_{i-1}^{j-1})^2, \quad i = 1, 2, ..., I \quad j = 1, 2, ..., J \tag{20}$$

The discrete point form of the initial condition is:

$$e_i^0 = e_0 \tag{21}$$

The discrete point forms of the single-sided drainage boundary conditions are:

$$e_{I+1}^j = e_0 \tag{22}$$

$$e_0^j = e_2^j - \frac{2\Delta a(\gamma_s - \gamma_f)}{1 + e_0}a_v^j \tag{23}$$

where, e_{I+1}^j and e_0^j represent the void ratio of the top and bottom boundaries at a certain time, respectively.

Putting Eqs. (21)-(23) into Eq. (20), the matrix form of Eq. (20) can be written as:

$$\begin{bmatrix} P_1 & 1 & & & & \\ 1 & P_2 & 1 & & & \\ & 1 & P_3 & 1 & & \\ & & \ddots & \ddots & \ddots & \\ & & & 1 & P_{I-1} & 1 \\ & & & & 1 & P_I \end{bmatrix}^{j-1} \begin{bmatrix} e_1 \\ e_2 \\ e_3 \\ \vdots \\ e_{I-1} \\ e_I \end{bmatrix}^j = \begin{bmatrix} Q_1 \\ Q_2 \\ Q_3 \\ \vdots \\ Q_{I-1} \\ Q_I \end{bmatrix} \tag{24}$$

where,

$$P_i = -2\left(1 + \frac{\Delta a^2}{\Delta t C_i^{j-1}}\right) \tag{25}$$

$$Q_1 = 2\left(1-\frac{\Delta a^2}{\Delta t C_1^{j-1}}\right)e_1^{j-1} - 3e_2^{j-1} - \frac{2\Delta a^2 A_1^{j-1}}{C_1^{j-1}}K_1^{j-1} - \frac{2\Delta a^2 B_1^{j-1}}{C_1^{j-1}}(K_1^{j-1})^2 + 4\Delta a K_1^{j-1} \tag{26}$$

$$Q_i = -e_{i+1}^{i-1} + 2\left(1-\frac{\Delta a^2}{\Delta t C_i^{j-1}}\right)e_i^{j-1} - e_{i-1}^{j-1} - \frac{\Delta a A_i^{j-1}}{C_i^{j-1}}(e_{i+1}^{j-1} - e_{i-1}^{j-1}) - \frac{B_i^{j-1}}{2C_i^{j-1}}(e_{i+1}^{j-1} - e_{i-1}^{j-1})^2 \tag{27}$$

$$Q_I = -2e_0 + 2\left(1-\frac{\Delta a^2}{\Delta t C_I^{j-1}}\right)e_I^{j-1} - e_{I-1}^{j-1} - \frac{\Delta a A_I^{j-1}}{C_I^{j-1}}(e_0 - e_{I-1}^{j-1}) - \frac{B_I^{j-1}}{2C_I^{j-1}}(e_0 - e_{I-1}^{j-1})^2 \tag{28}$$

As mentioned above, here K_1 is:

$$K_1 = \frac{\gamma_s - \gamma_f}{(1+e_0)}a_v \tag{29}$$

According to the initial conditions and the boundary conditions, the void ratio at a certain moment can be calculated by void ratio at the previous moment which has already been calculated. In addition, the correct selection of the segmented $e-\sigma'$ expressions in differential calculation can be realized by a judgment statement in every step. If the effective stress is smaller than the remolded yield stress, using the first relation in Eq. (2), otherwise, the second relation is adopted. While in the typical models, there is no need to make a choice. After a series of cycles, the void ratio at any point in the schematic diagram [Fig. 2] can be obtained.

Following Gibson et al. (1981), the average degree of consolidation calculated in this paper is defined by deformation, that is:

$$U_t = \frac{S_t}{S_\infty} = \frac{\int_0^{a_0}\left[e(a,0)-e(a,t)\right]\mathrm{d}a}{\int_0^{a_0}\left[e(a,0)-e(a,\infty)\right]\mathrm{d}a} \tag{30}$$

where, S_t is the settlement at time t; S_∞ is the total settlement when consolidation is completed. In the difference calculation, they are expressed as:

$$S_t = a_0 - \frac{1}{1+e_0}\left(a_0 + \sum_{i=1}^{I+1}\frac{e_i^j + e_{i-1}^j}{2}\Delta a\right) \tag{31}$$

$$S_\infty = a_0 - \frac{1}{1+e_0}\left(a_0 + \sum_{i=1}^{I+1}\frac{e_i^\infty + e_{i-1}^\infty}{2}\Delta a\right) \tag{32}$$

Model performance

Verification by CS2 model

The change law of void ratios on the height scale is a detailed description of the settlement process for a specific model, which can intuitively reflect where the soil consolidation mainly occurs at a certain state. For verification, the predicting process using CS2 is also shown in Fig. 3 to prove the accuracy of the solution calculated by FDM (Fox and Berles 1997; Fox and Pu 2012). The excellent agreement of these two solutions is observed in the results. As shown in Fig. 3, in the early stage of consolidation, the lower soil layers compress and settle while the upper soil layers basically remain unchanged. As time goes by, the void ratios of higher soil layers begin to decrease, and finally, the whole soil reaches a stable state. This reveals a mechanism of self-weight consolidation of dredged silt, starting from the bottom, where the effective stress increases faster.

Comparison with experimental and predicted settlement curves

Bartholomeeusen et al. (2002) conducted a typical settling column experiment to study the differences of several numerical models on predicting large-strain consolidation behavior of dredged soil. All the models adopted the Gibson large-strain equation as the basis of development. The permeability and compressibility relations used in these models are common types of semi-logarithmic and double-logarithmic. The detailed information of the participants in the comparison is shown in

Table 1. The soil sample has an initial void ratio of 2.52, a liquid limit of 39% and a specific gravity of 2.72, from the river Schelde, Belgium. Fig. 4 shows the results of these predictions along with the experimental observations. It is immediately apparent that all the solutions of the participants show too fast a consolidation process, with the majority of the settlement complete within 7 days. The presented model, on the other hand, suggests that settlement is still ongoing at 7 days, consistent with the measured data. Although a later measurement at 15 days showed that the settlement ceased at 0.410m (Bartholomeeusen et al. 2002), close to the values predicted by the participants, the end times of consolidation in the predictions are too early to be accepted. In practical engineering, overestimating the consolidation rate means that the bearing capacity of soil at this time does not meet the requirements of following operations, which is not allowed, especially for large-scale practices. Therefore, the presented model is proved to be the better option to describe the large-strain self-weight consolidation of slurries. The differences that exist among these models can generally be attributed to the differences in the correlations of permeability and compressibility. That's exactly what this article wants to explore.

Parametric analyses

The initial height, initial void ratio, void ratio at liquid limit and specific gravity of soil particles are considered to be the main factors affecting soil's consolidation process in this model. To statistically observe how these parameters affect the consolidation process, nine sets of parameters shown in Table 2 were adopted in the following calculation. The values of the parameters selected in these nine groups above meet the requirements proposed by Hong et al. (2010), which limits the value

ranges of ω_0 to 50%-146% and ω_L to 42%-106%.

Meanwhile, since the typical constitutive models have more simple forms and are still commonly used to analyze the consolidation behavior of dredged soil (Feng et al. 2019; Pu et al. 2020), comparisons are made to explore the deviation between different constitutive models. The standard forms of the classical semi-logarithmic and double-logarithmic models are given here, which are very concise, only containing void ratio, permeability coefficient, effective stress and some constants, and are convenient to obtain by simple compression and permeability tests.

semi-logarithmic model

$$e = a_1 \ln(\sigma') + b_1 \tag{33}$$

$$e = c_1 \ln(k) + d_1 \tag{34}$$

double-logarithmic model

$$e = a_2 (\sigma')^{b_2} \tag{35}$$

$$k = c_2 e^{d_2} \tag{36}$$

where, a_1, b_1, c_1, d_1, a_2, b_2, c_2, and d_2 are all constants, varying with different calculation examples. It should be pointed out that, in this article, the parameters in the typical models were determined by fitting Cao et al.'s (2014) model (i.e. experiment curves), units in m/s and kPa.

The effect of initial height

The influences of soils' initial heights (H) on self-weight consolidation are shown in Figs. 5(a)-5(c). The soils in Groups 1, 2 and 3 have the same parameter values except for the initial heights, which are 10m, 15m, and 20m respectively. Take the solutions adopting Cao et al.'s (2014) model (SCM) as an example to analyze the influence of initial height on the settlement process of dredged slurries.

246 When the consolidation is completed, the final void ratios at the bottom of the soils for the three groups
247 are 1.558, 1.445 and 1.368, respectively. And clearly, the greater initial height leads to a smaller final
248 void ratio along the whole normalized depth, which means the soil becomes denser and stronger. From
249 the distribution curves of the final void ratio shown in Fig. 5(a), the non-linear variation of the void
250 ratio is extremely obvious on the height scale. The void ratio decreases as the height drops, while the
251 void ratio of the top layer keeps constant and equals the initial void ratio. In comparison, the void ratio
252 changes between the upper soil layers are more evident than that of the lower soil layers. For example,
253 from the surface to the relative height of 0.8 of the soil sample, the void ratio decreases by more than
254 60%. From the relative height of 0.8 to the bottom, the void ratio shows a relatively small change. This
255 is the result of the apparent nonlinear $e-\sigma'$ relationship of the sludge. The compressibility decreases
256 with the increase of the effective stress. Thus, the subsoils with greater effective stress change less in
257 the void ratio.

258 The total settlements of the three groups are 3.254m, 5.287m and 7.428m, and the corresponding
259 vertical strains are 32.54%, 35.25% and 37.14% respectively, which increase with the increase of the
260 initial heights. In the aspect of consolidation speed, the times required to complete 90% of the
261 consolidation for the three groups are 43.693a, 74.993a and 109.09a, respectively [Fig. 5(c)]. The
262 impact of initial height on the consolidation speed is significant. From the results it can be known that
263 the soil sample with a higher initial height has a larger final relative settlement, a greater final average
264 void ratio, and a lower consolidation speed. This conclusion is also observed in the solutions adopting
265 the semi-logarithmic model (SSM) and the solutions adopting the double-logarithmic model (SDM),
266 though the consolidation processes are different from each other.

Compared with SSM and SDM, the final void ratios at the bottom layers of SCM are 0.970, 0.982 and 0.996 times that of SSM, 0.909, 0.903 and 0.899 times that of SDM respectively. The total settlements of SCM are 1.065, 1.045 and 1.032 times that of SSM, 1.237, 1.203 and 1.183 times that of SDM respectively. Following the distribution of the curves in Figs. 5(a)-5(c) and the changing trends of the ratios calculated above, some interesting points could be found. In general, under the same parameter setting, the final average void ratio of SCM is the lowest, corresponding to the largest total settlement. The value of the final average void ratio of SSM is between SCM and SDM, and so is the total settlement. As the initial height increases, the differences of the final average void ratio and total settlement between each of them decrease. In terms of consolidation rate, the consolidation of SCM is the fastest all the time. The consolidation of SDM is the slowest in the early stage of consolidation, but that of SSM becomes the slowest when the degree of consolidation is greater than about 75%.

Besides, the changing trends of the settlement and consolidation curves show a clearly fast first and slow afterward type for all the three solutions. Theoretically, there should be an inflection point corresponding to the remolded yield stress σ_s' on the settlement curve because of the segmented $e-\sigma'$ relationships in Cao et al.'s (2014) model. Unexpectedly, it is not visible in the above settlement curves until parts of them are magnified hundreds of times [Fig. 5(b)], which indicates that there is no significant difference in the law of void ratio change on both sides of the remolded yield stress. It's a proof that these two piecewise functions are smoothly connected.

The effect of initial void ratio

Figs. 6(a)-6(c) reveal how the initial void ratio (e_0) affects the self-weight consolidation process of dredged sludge. The only difference for parameters of soils in Groups 4, 3 and 5 is controlled to be

288 e_0, which are 2.4, 3.2, and 4.0, respectively. Analyzing the SCM separately, at the end of consolidation,
289 the final void ratios are 1.306, 1.368 and 1.415 at the bottom of the soils for these three groups,
290 respectively. The total settlements are 5.015m, 7.428m and 9.212m, which account for 25.08%, 37.14%
291 and 46.06% of the soils' initial heights, respectively. The ratios increase with the increase of e_0. With
292 regard to consolidation speed, the times required to complete 90% of the consolidation are 195.987a,
293 109.09a and 69.083a, respectively. Consolidation develops more rapidly for the soil with a higher
294 initial void ratio. Overall, higher e_0 leads to bigger final average void ratio, greater total settlement,
295 and higher consolidation speed.

296 Compared with SSM, the final void ratios at the bottom layers of SCM are 0.975, 0.996 and 1.019
297 times that of SSM, respectively. This reveals that depending on the value of e_0, the final void ratio at
298 the bottom layer of SSM can either be bigger or smaller than that of SCM. Whereas, the corresponding
299 total settlement of SCM shown in Fig. 6(b) is always greater than that of SSM, because the spatial
300 distributions of the final void ratios calculated by the two models are different as shown in Fig. 6(a).
301 For SDM, the final void ratios at the bottom layers of SCM are 0.896, 0.899 and 0.901 times that of
302 SDM respectively. The total settlements of SCM are 1.287, 1.183 and 1.151 times that of SDM
303 respectively. As e_0 increases, the differences of the final average void ratio and total settlement
304 between SCM and SDM decrease. Concerning consolidation speed, as shown in Fig. 6(c), the change
305 process of the three solutions' relative relationship is complicated. When e_0 is 2.4, the consolidation
306 of SCM is the fastest, and that of SSM is the slowest. As e_0 increases, the consolidation of SSM
307 becomes the fastest in the early stage of consolidation, then slows down to be the slowest when the
308 degree of consolidation is greater than about 70%.

309 ***The effect of void ratio at liquid limit***

310 In this section, the effect of the void ratio at liquid limit (e_L) of dredged sludge on the self-weight
311 consolidation is investigated as shown in Figs. 7(a)-7(c). The soils in Groups 6, 3 and 7 have the same
312 parameter values except for e_L , which are 1.62, 2.16, and 2.70 respectively. Firstly, discussing the
313 SCM individually, when the consolidation is completed, the final void ratios are 1.078, 1.368 and 1.661
314 at the bottom of the soils for these three groups, respectively. The total settlements are 9.155m, 7.428m
315 and 5.798m, which account for 45.78%, 37.14% and 28.99% of the initial heights of the soils,
316 respectively. The ratios decrease with the increase of e_L , agreeing excellently with the increase of the
317 final average void ratios. In terms of consolidation speed, the times required to complete 90% of the
318 consolidation are 46.081a, 109.09a and 212.42a, respectively. It can be concluded that consolidation
319 develops slower for a higher e_L . Besides, it is worth mentioning that there is a big difference of
320 remolded yield stresses for three groups in this section as shown in Fig. 7(b), which indirectly proves
321 that e_L plays an important role in Cao et al.'s (2014) model.

322 Making a comparison of the three solutions, the final void ratios at the bottom layers of SCM are
323 1.200, 0.996 and 0.979 times that of SSM, respectively. The total settlements of SCM are 0.986, 1.032
324 and 0.984 times that of SSM, which means the total settlement of SSM is larger than that of SCM
325 when e_L is small or big enough. The settlement relationship between SCM and SSM deviates from
326 their relationship of final void ratio at the bottom layer, which indicates that the two solutions have
327 different void ratio distribution rules, as shown in Fig. 7(a). For SDM, the final void ratios at the bottom
328 layers of SCM are 0.904, 0.899 and 0.929 times that of SDM respectively. The total settlements of
329 SCM are 1.140, 1.183 and 1.140 times that of SDM respectively. It is conceivable that, as e_L

increases from 1.62 to 2.70, the differences of final average void ratio and total settlement between SCM and SDM have maximum values respectively. In terms of consolidation rate, the consolidation of SHD is the fastest in general. For different values of e_L, the relative consolidation speed of SSM and SDM always changes in the middle stage of consolidation. The faster one in the first half is SSM.

The effect of specific gravity of soil particles

Keeping the initial void ratio and other parameters unchanged, different specific gravities of soil particle (G_s) were set as 2.6, 2.7 and 2.8 (for groups 8, 3 and 9) to predict the soil consolidation process. The results are obtained, as shown in Figs. 8(a)-8(c). For the SCM, at the end of consolidation, the final void ratios are 1.384, 1.368 and 1.353 at the bottom of the soils for these three groups, respectively. The total settlements are 7.344m, 7.428m and 7.506m, which account for 36.72%, 37.14% and 37.53% of the initial heights of the soils, respectively. The ratios increase slightly with the increase of G_s. In the aspect of consolidation speed, the times required to complete 90% of the consolidation are 114.624a, 109.09a and 105.983a, respectively. The conclusion is that the higher the G_s is, the smaller the final average void ratio is. And, the final settlement is greater and consolidation is faster for the soil sample with a higher G_s.

The curves in the Figs. 8(a)-8(c) show that for a particular model, the impact of G_s on the final void ratio's distribution, settlement and consolidation process is much subtler, relative to the initial height, initial void ratio, and void ratio at liquid limit. On the other hand, under the same parameter settings, the differences of final void ratio's distribution, settlement and consolidation process among the three solutions are much more obvious. Briefly speaking, the total settlement of SCM is the largest, followed by SSH. In terms of consolidation speed, there is little difference between each of the three

351 solutions.

352

353 ## Discussion

354 The permeability and compressibility relations play essential roles in predicting the soil's
355 consolidation behavior, and largely affect the validities of the models. The constitutive relations used
356 in the presented model was proposed based on series of tests on dredged soils with high water contents.
357 Soil properties, including e_0, e_L, σ_s', C_c^* and e_{100}^*, which are not involved in the conventional
358 models, express the particularity of this model. Comparing the experimental observations with
359 numerical predictions of the dredged material's settlement behavior, results indicate that the
360 consolidation processes predicted by the traditional models are much faster and the final settlements
361 are greater than the actual situation. In contrast, the presented model is in good agreement with the
362 measurements in Bartholomeeusen et al. (2002).

363 Generally, according to the parametric analyses, the conventional logarithmic models would
364 underestimate the consolidation rate and the final settlement compared with the presented model,
365 although in some cases the results turn out to be the opposite. However, for a short period at the
366 beginning of consolidation, the consolidation process predicted by the presented model is always
367 slower than that of the typical models, just the same as the law found in Fig. 4. This reveals that the
368 settlement process in Bartholomeeusen et al. (2002) is not completed within 7 days, or even after 15
369 days. The literature data also suggests that the settlement in a few days only accounts a small part of
370 the self-weight consolidation of soft soils (Mcvay et al. 1986; Ito and Azam 2013).

371 Besides, the semi-logarithmic and double-logarithmic models react more sensitive to the changes

of these parameters, especially when the analysis variables in the examples are not involved in their models, such as initial void ratio and void ratio at liquid limit. Their performance instability may be attributed to the universality and simplicity of the typical relations, which leads to the deduction of effectiveness when applied to different soil samples. The presented model, proposed especially for studying the consolidation characteristics of dredged soil, avoids this problem commendably.

Conclusion

A large-strain self-weight consolidation model of dredged sludge was built considering the special non-linear permeability and compressibility of soil with high water content. The highly nonlinear equation was solved by the FDM in Crank-Nicolson format. The consolidation behavior under the special constitutive model was analyzed by comparing it with the conventional semi-logarithmic and double-logarithmic models under different parameter settings. Some detailed conclusions are given as follows:

1 Self-weight consolidation considering non-linear permeability and compressibility often takes decades or even hundreds of years to complete. At the end of consolidation, from the surface to the relative height of 0.8 of the soil sample, the void ratio decreases by more than 60%, even by 85% in some cases. From the relative height of 0.8 to the bottom, the void ratio shows a relatively small change.

2 The sludge with a higher specific gravity of soil particles or initial void ratio has a larger settlement and a higher consolidation speed. The sludge with a greater initial height has a larger relative settlement but a lower consolidation speed. On the contrary, the sludge with a higher void ratio at liquid limit would get a smaller settlement and a lower consolidation rate.

3 Comparing the changes of final void ratio's distributions, settlement and consolidation processes in the analyses of the four parameters, it can be concluded that the self-weight consolidation of dredged sludge is most sensitive to the void ratio at liquid limit, and its response to the change of specific gravity is subtle.

4 In terms of settlement, the total settlement of SCM is the largest, and that of SDM is the smallest. When the value of void ratio at liquid limit is too small or too big, such as 1.62 and 2.70 in this paper, the total settlement of SSM is larger than that of SCM. As the initial height and initial void ratio increase, the differences of total settlements among the three solutions decrease.

5 As for consolidation rate, the consolidation of SCM is the fastest. Compared with SCM, the consolidation of SSM is rapid in the early stage, even faster than that of SCM in some cases, but slows down to be the slowest in the later stage until consolidation is completed. SDM is the opposite of SSM.

6 Generally, compared with SCM, SSM and SDM would underestimate the consolidation rate and the final settlement, though it turns out to be the opposite at the very beginning of consolidation. Besides, due to the generality and simplicity of the semi-logarithmic and double-logarithmic models, the accuracy of their description of the consolidation characteristics of a specific soil type is weakened. Especially when the analysis variables in the examples are not involved in the models, such as initial void ratio and void ratio at liquid limit, their effectiveness is further reduced. The present model is proposed for dredged sludge, considering several important soil parameters. It is more accurate and stable in analyzing the consolidation characteristics of dredged sludge.

Data Availability Statement

All data, models, and code generated or used during the study appear in the submitted article.

Acknowledgments

The work described in this paper was supported by the Key Research and Development Project of Chinese Ministry of Science and Technology (Grant No. 2017YFE0119500), National Natural Science Foundation of China (Grant Nos. 52078464, 51978621, 51620105008), European Union's Horizon 2020 MARIE SKŁODOWSKA-CURIE RESEARCH AND INNOVATION STAFF EXCHANGE Program (Grant No. 778360), National Key R&D Program of China (2016YFC0800200), and Key R&D Program of Zhejiang Province (Grant No. 2018C03038). The authors are very grateful for the above supports.

Notation

The following symbols are used in this paper:

a = space coordinate;

a_v = coefficient of compressibility;

a_0 = total thickness of the soil sample in the FDM model;

E_0 = the intercept of the compression curve on the longitudinal axis;

e = void ratio;

e_i^j = void ratio of the top of ith sublayer at time $j\Delta t$;

e_L = void ratio at liquid limit;

e_s = void ratio corresponding to remolded yield stress;

e_0 = initial void ratio;

436 e_{100}^{*} = void ratio of the reconstituted clays at the effective vertical stress of 100 kPa;

437 G_s = specific gravity of soil particles;

438 H = initial height of soil sample;

439 I = numbers of sublayers in the FDM model;

440 i = ith element, space direction;

441 J = numbers of time periods in the FDM model;

442 j = jth element, time direction;

443 k = coefficient of vertical permeability;

444 k_j = coefficient of vertical permeability at time $j\Delta t$;

445 k_s = coefficient of vertical permeability corresponding to remolded yield stress;

446 k_0 = initial coefficient of vertical permeability;

447 m_v = the volume compressibility coefficient;

448 n = the slope of the compression curve;

449 p = the vertical pressure;

450 S = settlement;

451 S_t = settlement at time t;

452 S_∞ = total settlement when consolidation is completed;

453 t = time;

454 U_t = degree of consolidation at time t;

455 u = excessive pore water pressure;

456 z = height of a certain soil layer;

457 Δa = thickness of ecah sublayer in the FDM model;

458 Δt = length of the each time period in the FDM model;

459 α = constant;

460 γ_s = gravity of solid;

461 γ_f = gravity of fluid;

462 ε = vertical compressive strain;

463 ξ = convective coordinate changing with a and t;

464 σ' = vertical effective stress;

465 σ_0' = initial vertical effective stress;

466 σ_j' = vertical effective stress at time $j\Delta t$;

467 σ_s' = remolded yield stress;

468 σ_{si}' = remolded yield stress for soil group i ;

469 ω_0 = initial water content;

470 ω_L = water content at liquid limit.

471

472 **References**

473 Al-Furjan, M. S. H., Habibi, M., Ghabussi, A., Safarpour, H., Safarpour, M., and Tounsi, A. (2020a).

474 "Non-polynomial framework for stress and strain response of the FG-GPLRC disk using three-

475 dimensional refined higher-order theory." *Eng. Struct.*, 228, 111496.

476 https://doi.org/10.1016/j.engstruct.2020.111496.

477 Al-Furjan, M. S. H., Habibi, M., Jing, N., Dong, W. J., and Tounsi, A. (2020b). "Frequency simulation

of viscoelastic multi-phase reinforced fully symmetric systems." *Eng. Comput.*, (11), 1-17. https://doi.org/10.1007/s00366-020-01200-x.

Al-Furjan, M. S. H., Habibi, M., Rahimi, A., Chen, G., and Tounsi, A. (2020c). "Chaotic simulation of the multi-phase reinforced thermo-elastic disk using GDQM." *Eng. Comput.*, (1). https://doi.org/10.1007/s00366-020-01144-2.

Al-Furjan, M. S. H., Hatami, A., Habibi, M., Shan, L., and Tounsi, A. (2020d). "On the vibrations of the imperfect sandwich higher-order disk with a lactic core using generalize differential quadrature method." *Compos. Struct.*, 257, 113150. https://doi.org/10.1016/j.compstruct.2020.113150.

Al-Furjan, M. S. H., Safarpour, H., Habibi, M., Safarpour, M., and Tounsi, A. (2020e). "A comprehensive computational approach for nonlinear thermal instability of the electrically FG-GPLRC disk based on GDQ method." *Eng. Comput.*, (2). https://doi.org/10.1007/s00366-020-01088-7.

Alimirzaei, S., Mohammadimehr, M., and Tounsi, A. (2019). "Nonlinear analysis of viscoelastic micro-composite beam with geometrical imperfection using FEM: MSGT electro-magneto-elastic bending, buckling and vibration solutions." *Struct. Eng. Mech.*, 71(5), 485-502. https://doi.org/10.12989/sem.2019.71.5.485.

Barden, L. (1965). "Consolidation of Clay with Non-linear Viscosity." *Géotechnique*, 15(4), 345–362. https://doi.org/10.1680/geot.1965.15.4.345.

Barden, L., and Berry, P. L. (1965). "Consolidation of normally consolidated clay." *Journal of Soil Mechanics & Foundations Div*, 95(1), 15-35. https://doi.org/10.1061/JSFEAQ.0000790.

Bartholomeeusen, G., Sills, G. C., Penumadu, D., Carrier, W. D., Masala, S., and Chan, D. (2002).

Sidere: numerical prediction of large-strain consolidation. *Géotechnique*, 52(9), 639-648. https://doi.org/10.1680/geot.2002.52.9.639.

Cargill, K. W. (1984). "Prediction of consolidation of very soft soil." *J. Geotech. Eng.*, 110(6), 775-795. https://doi.org/10.1061/(ASCE)0733-9410(1984)110:6(775).

Cao, Y. P., Wang, X. S., Du, L., Ding, J. W., and Deng, Y. F. (2014). "A method of determining nonlinear large strain consolidation parameters of dredged clays." Water Science and Engineering. 7(2), 218-226. https://doi.org/10.3882/j.issn.1674-2370.2014.02.009.

Chai, J. C., Horpibulsuk, S., Shen, S. L., and Carter, J. P. (2014). "Consolidation analysis of clayey deposits under vacuum pressure with horizontal drains." *Geotext. Geomembr.*, 42, 437–444. http://dx.doi.org/10.1016/j.geotexmem.2014.07.001.

Davis, E. H., and Raymond, G. P. (1965). "A non-linear theory of consolidation." *Géotechnique*, 15(2), 161-173. https://doi.org/10.1680/geot.1965.15.2.161.

Du, C., Zhang, J., Zhang, T., and Yang, Q. (2019). "Effect of salt on strength development of marine soft clay stabilized with cement-based composites." *Mar. Geores. Geotechnol.*, (4), 1-14. https://doi.org/10.1080/1064119X.2019.1612971.

Ekolin, G. (1991). "Finite difference methods for a nonlocal boundary value problem for the heat equation." *Bit*. 31(2), 245-261. https://doi.org/10.1007/BF01931285.

Feng, J., Ni, P. P., and Mei, G. X. (2019). "One-dimensional self-weight consolidation with continuous drainage boundary conditions: solution and application to clay-drain reclamation." *Int. J. Numer. Anal. Methods Geomech.*, 43(8), 1634-1652. https://doi.org/10.1002/nag.2928.

Fox, P. J., and Berles, J. D. (1997). "Cs2: a piecewise-linear model for large strain consolidation." *Int.*

J. Numer. Anal. Methods Geomech., 21, 453-475. https://doi.org/10.1002/(SICI)1096-9853(199707)21:7<453::AID-NAG887>3.0.CO.

Fox, P. J., and Pu, H. (2012). "Enhanced cs2 model for large strain consolidation." *Int. J. Geomech.*, 12(5), 574-583. https://doi.org/10.1061/(ASCE)GM.1943-5622.0000171.

Gibson, R. E., England, G. L., and Hussey, M. J. L. (1967). "The theory of one-dimensional consolidation of saturated clays: 1. finite non-linear consolidation of thin homogeneous layers." *Géotechnique*, 17(3), 261-273. https://doi.org/10.1680/geot.1967.17.3.261.

Gibson, R. E., Schiffman, R. L., and Cargill, K. W. (1981). "The theory of one-dimensional consolidation of saturated clays. ii. finite nonlinear consolidation of thick homogeneous layers." *Can. Geotech. J.*, 18(2), 280-293. https://doi.org/10.1139/t81-030.

Hansbo, S. (1960). "Consolidation of clay with special reference to influence of vertical sand drains." Swedish Geotechnical Institute. 18, 45–50.

Hawlader, B. C., Muhunthan, B., and Imai, G. (2008). "State-dependent constitutive model and numerical solution of self-weight consolidation." *Géotechnique*, 58(2), 133-141. https://doi.org/10.1680/geot.2008.58.2.133.

He, J., Shi, X. K., Li, Z. X., Zhang, L., Feng, X. Y., and Zhou, L. R. (2020). "Strength properties of dredged soil at high water content treated with soda residue, carbide slag, and ground granulated blast furnace slag." *Constr. Build. Mater.*, 242, 118126. https://doi.org/10.1016/j.conbuildmat.2020.118126.

Hirian, H., Belarbi, M. O., Houari, M., Houari, M. S. A., and Tounsi, A. (2021). "On the layerwise finite element formulation for static and free vibration analysis of functionally graded sandwich plates." *Eng. Comput.*, (3), 3. https://doi.org/10.1007/s00366-020-01250-1.

Hong, Z. S., Yin, J., Cui, Y. J. (2010). "Compression behavior of reconstituted soils at high initial water contents." *Géotechnique*, 60(9), 691--700. https://doi.org/10.1680/geot.09.P.059.

Ito, M., and Azam, S. (2013). "Large-strain consolidation modeling of mine waste tailings." *Environmental Systems Research*, 2(7), 1-12. https://doi.org/10.1186/2193-2697-2-7.

Kessel, T. V., and Kesteren, W. G. M. V. (2002). "Gas production and transport in artificial sludge depots." *Waste Manage*., 22(1), 19-28. https://doi.org/10.1016/S0956-053X(01)00021-6.

Lang, L., Chen, B., and Li, N. (2020a). "Utilization of lime/carbide slag-activated ground granulated blast-furnace slag for dredged sludge stabilization." *Mar. Geores. Geotechnol*., 1-11. https://doi.org/10.1080/1064119X.2020.1741050.

Lang, L., Liu, N., and Chen, B. (2020b). "Investigation on the strength, durability and swelling of cement- solidified dredged sludge admixed fly ash and nano-SiO2. *Eur. J. Environ. Civ. Eng*., 1-21. https://doi.org/10.1080/19648189.2020.1776160.

Lang, L., Chen, B., and Chen, B. (2021). "Strength evolutions of varying water content-dredged sludge stabilized with alkali-activated ground granulated blast-furnace slag." *Constr. Build. Mater*., 275, 122111. https://doi.org/10.1016/j.conbuildmat.2020.122111.

Lee, K., and Sills, G. C. (2010). "The consolidation of a soil stratum, including self-weight effects and large strains." *Int. J. Numer. Anal. Methods Geomech*., 5(4), 405-428. https://doi.org/10.1002/nag.1610050406.

Mesri, G., and Rokhsar, A. (1974). "Theory of consolidation for clays." *J. Geotech. Eng*., 100(8), 889-904.

McNabb, A. (1960). "A mathematical treatment of one-dimensional soil consolidation." *Q. Appl.*

562 *Math*., 17(4), 337-347. https://doi.org/10.1090/qam/113405.

563 Mikasa, M. (1965). "The consolidation of soft clay-a new consolidation theory and its application."

564 Equations. Tokyo, Japan: Kajima Institute Publishing Co., Ltd. 21-26.

565 Mcvay, M., Townsend, F., and Bloomquist, D. (1986). "Quiescent consolidation of phosphatic waste

566 clays." *J. Geotech. Eng*., 112(11), 1033-1049.

567 https://doi.org/10.1061/(ASCE)0733-9410(1986)112:11(1033).

568 Poskitt, T. J. (1969). "The consolidation of saturated clay with variable permeability and

569 compressibility." *Géotechnique*, 19(2), 234-252. https://doi.org/10.1680/geot.1969.19.2.234.

570 Papanicolaou, A. N., and Diplas, P. (1999). "Numerical solution of a non-linear model for self-weight

571 solids settlement." *Appl. Math. Model*., 23, 345-362.

572 https://doi.org/10.1016/S0307904X(98) 10092-6.

573 Peters G. P., and Smith D. W., (2002). "Solute transport through a deforming porous medium." *Int. J.*

574 *Numer. Anal. Methods Geomech*., 26, 683-717. https://doi.org/10. 1002/nag.219.

575 Pu, H. F., Wang, K., Qiu, J. W., and Chen, X. L. (2020). "Large-strain numerical solution for coupled

576 self-weight consolidation and contaminant transport considering nonlinear compressibility and

577 permeability." *Appl. Math. Model*., 88, 916-932. https://doi.org/10.1016/j.apm. 2020.07.010.

578 Rujikiatkamjorn, C., Indraratna, B., and Chu, J. (2007). "Numerical modelling of soft soil stabilized

579 by vertical drains, combining surcharge and vacuum preloading for a storage yard." *Can. Geotech.*

580 *J*., 44(3), 326-342(17). https://doi.org/10.1139/T06-124.

581 Schiffman, R. L. (1958). "Consolidation of soil under time-dependent loading and varying

582 permeability." Proceedings of the Thirty-Seventh Annual Meeting of the Highway Research Board. 37,

584–617.

Schiffman, R. L., McArthur, J. M., and Gibson, R. E. (1994). “Consolidation of clay layer: hydrogeologic boundary conditions.” *J. Geotech. Eng.*, 120(6), 1089-1093. https://doi.org/10.1061/(ASCE)0733-9410(1994)120:6(1089).

Terzaghi, K. (1924). “Die Theorie der Hydrodynamischen Spannungserscheinungen und ihr Erdbautechnisches Awendunsgebiet.” Proceedings of the First International Congress of Applied Mechanics. 1, 288–294.

Van Kessel, T., and Van Kesteren, W. G. M. (2002). Gas production and transport in artificial sludge depots. *Waste Management* 22(1), 19-28. https://doi.org/10.1016/S0956-053X(01)00021-6.

Wang, D., Di, S., Gao, X., Wang, R., and Chen, Z. (2020). “Strength properties and associated mechanisms of magnesium oxychloride cement-solidified urban river sludge.” *Constr. Build. Mater.*, 250(4), 118933. https://doi.org/10.1016/j.conbuildmat.2020.118933.

Wang, H. S., Tang, C. S., Gu, K., Shi, B., and Inyang, H. I. (2019). “Mechanical behavior of fiber-reinforced, chemically stabilized dredged sludge.” *Bull. Eng. Geol. Environ.*, 79(2), 629–643. https://doi.org/10.1007/s10064-019-01580-5.

Wang, L., Sun, J. S., Zhang, M. S., Yang, L. J., Li, L., and Yan, J. H. (2020). “Properties and numerical simulation for self-weight consolidation of the dredged material.” *Eur. J. Environ. Civ. Eng.*, 24(7), 949-964. https://doi.org/10.1080/19648189.2018.1432508.

Wei, R. L. (1993). “Derivation for Coefficient of Consolidation from Settlement Observation.” Chinese Journal of Geotechnical Engineering. 15(2), 12-19.

Xie, X. Y., Zhang, J. F., and Zeng, G. X. (2005). “Similarity solution of self-weight consolidation

problem for saturated soil." *Appl. Math. Mech.*, 26(9), 63-69. https://doi.org/CNKI:SUN:YYSL.0.2005-09-008.

Yao, D. T. C., Oliveira-Filho, W. L. D., Cai, X. C., and Znidarcic, D. (2002). "Numerical solution for consolidation and desiccation of soft soils." *Int. J. Numer. Anal. Methods Geomech.*, 26(2), 139-161. https://doi.org/10.1002/nag.196.

Tables

Table 1. Details of the participants in the comparison (units in kPa and m/s unless noted otherwise)

Participants	Mode types	Constitutive models
Bartholomeeusen (Bartholomeeusen et al. 2002)	Double-log & Semi-log	$e = -1.07\sigma'^{0.14} + 2.52$ $e = 0.27\ln(k) + 5.95$
Lin and Penumadu (Bartholomeeusen et al. 2002)	Semi-log & Double-log	$e = -0.22\ln(\sigma') + 1.46$ $k = 0.0072e^{6.75}$
Masala and Chan (Bartholomeeusen et al. 2002)	Double-log	$e = 2.81[\mathrm{Pa}^{-1}]\sigma'^{-0.102}$ $k = 1.38\times10^{-3}\,\mathrm{m/day}\ e^{5.75}$
Van Kessel (Van Kessel and Van kesteren 2002)	Semi-log (Natural exponential)	$\sigma' = \exp(11.27 - 8.0\ e)$ $k = \exp(-21.55 + 3.6\ e)$

Table 2. Basic physical properties of dredged slurries

Soil group	Initial height, H (m)	Initial void ratio, e_0	Void ratio at liquid limit, e_L	Specific gravity of soil particles, G_s (Mg/m^3)
1	10.0	3.2	2.16	2.7
2	15.0	3.2	2.16	2.7
3	20.0	3.2	2.16	2.7
4	20.0	2.4	2.16	2.7
5	20.0	4.0	2.16	2.7
6	20.0	3.2	1.62	2.7
7	20.0	3.2	2.70	2.7

8	20.0	3.2	2.16	2.6
9	20.0	3.2	2.16	2.8

614

615 **Figures**

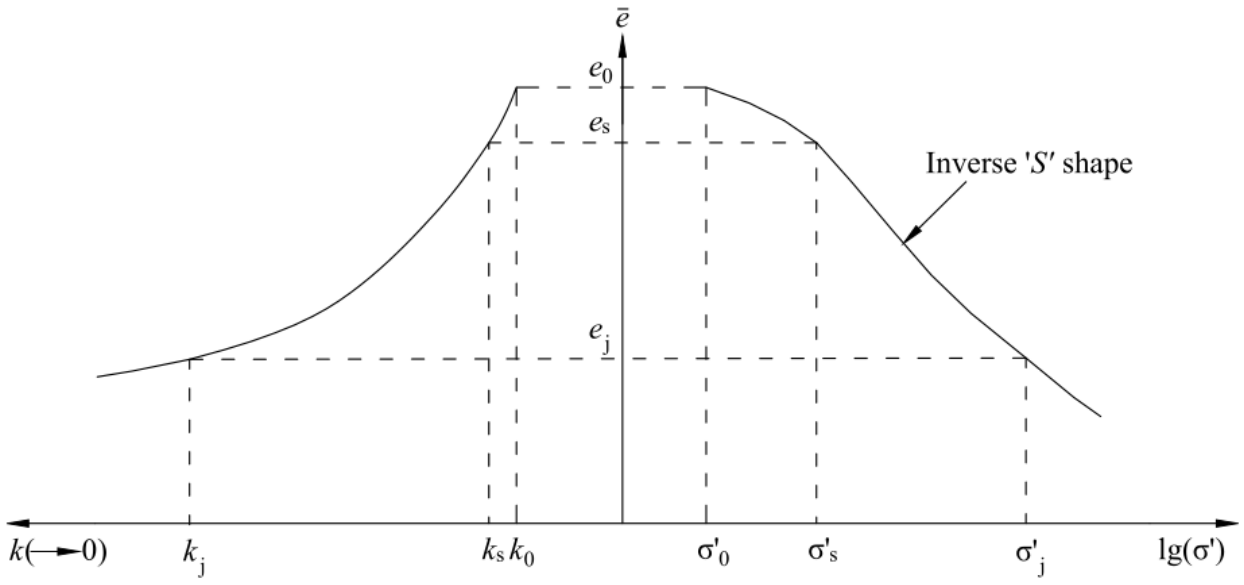

616

617 **Fig. 1.** Sketch map of the *e*-*k* and *e*-*σ′* relationships of Cao et al. (2014)

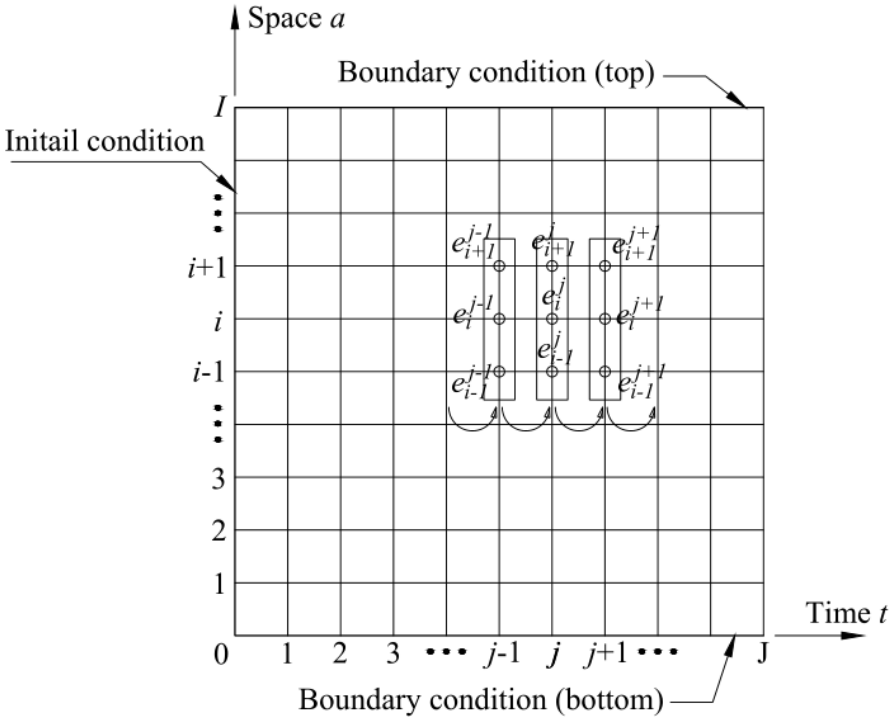

618

619 **Fig. 2.** Schematic diagram of finite difference

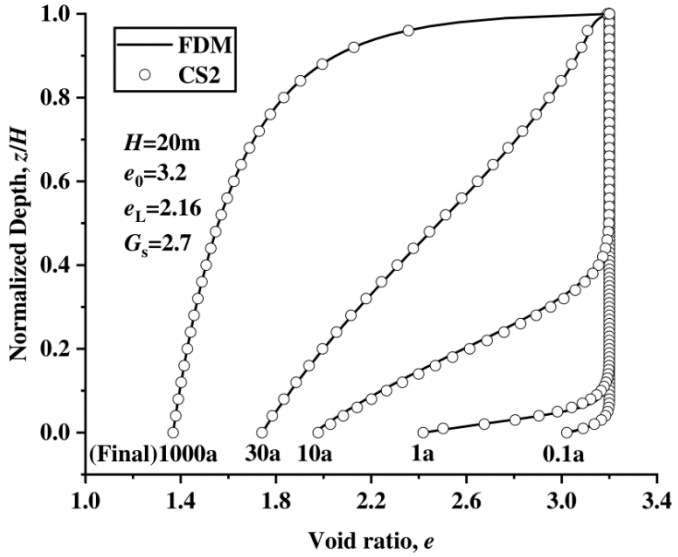

620

621 **Fig. 3.** Evolution of the distributions of void ratio in normalized height over times

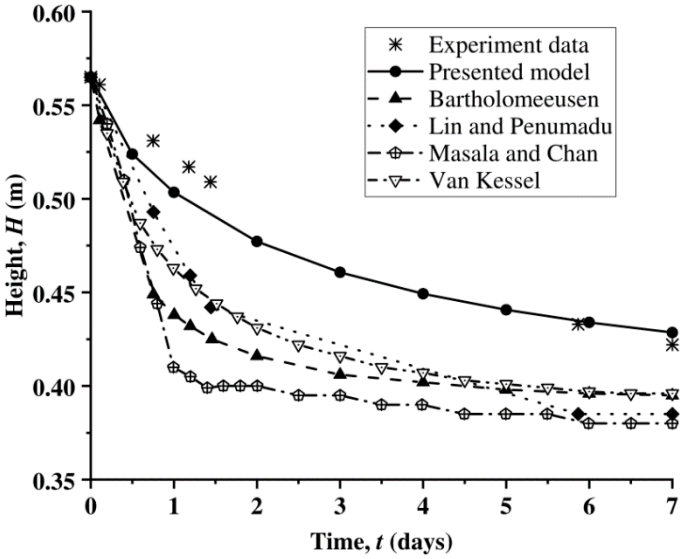

622

623 **Fig. 4.** Comparison of experimental and predicted settlement curves

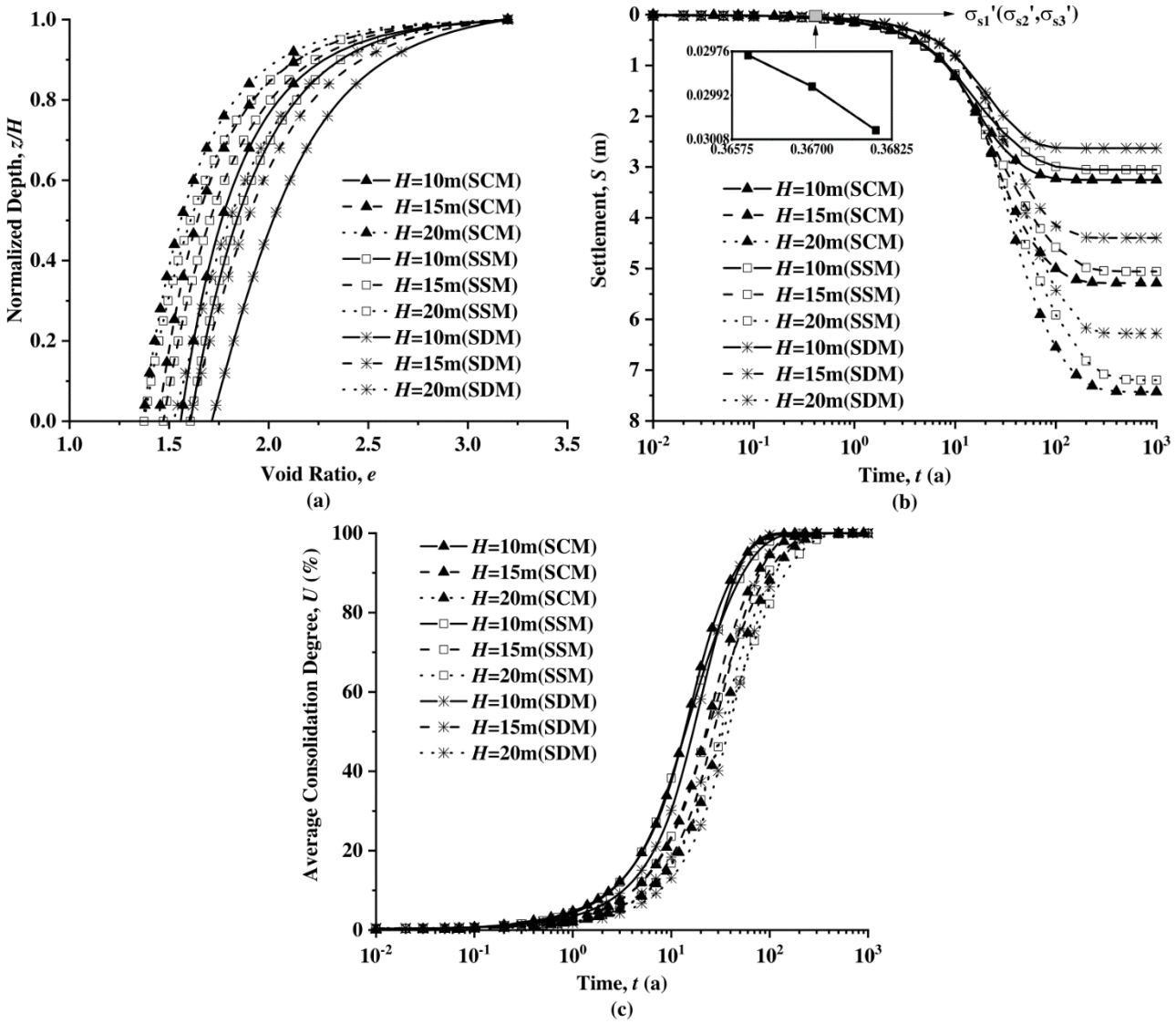

Fig. 5. Consolidation behavior of dredged sludge for different initial heights: (a) Final void ratio distribution; (b) Settlement; (c) Average consolidation degree

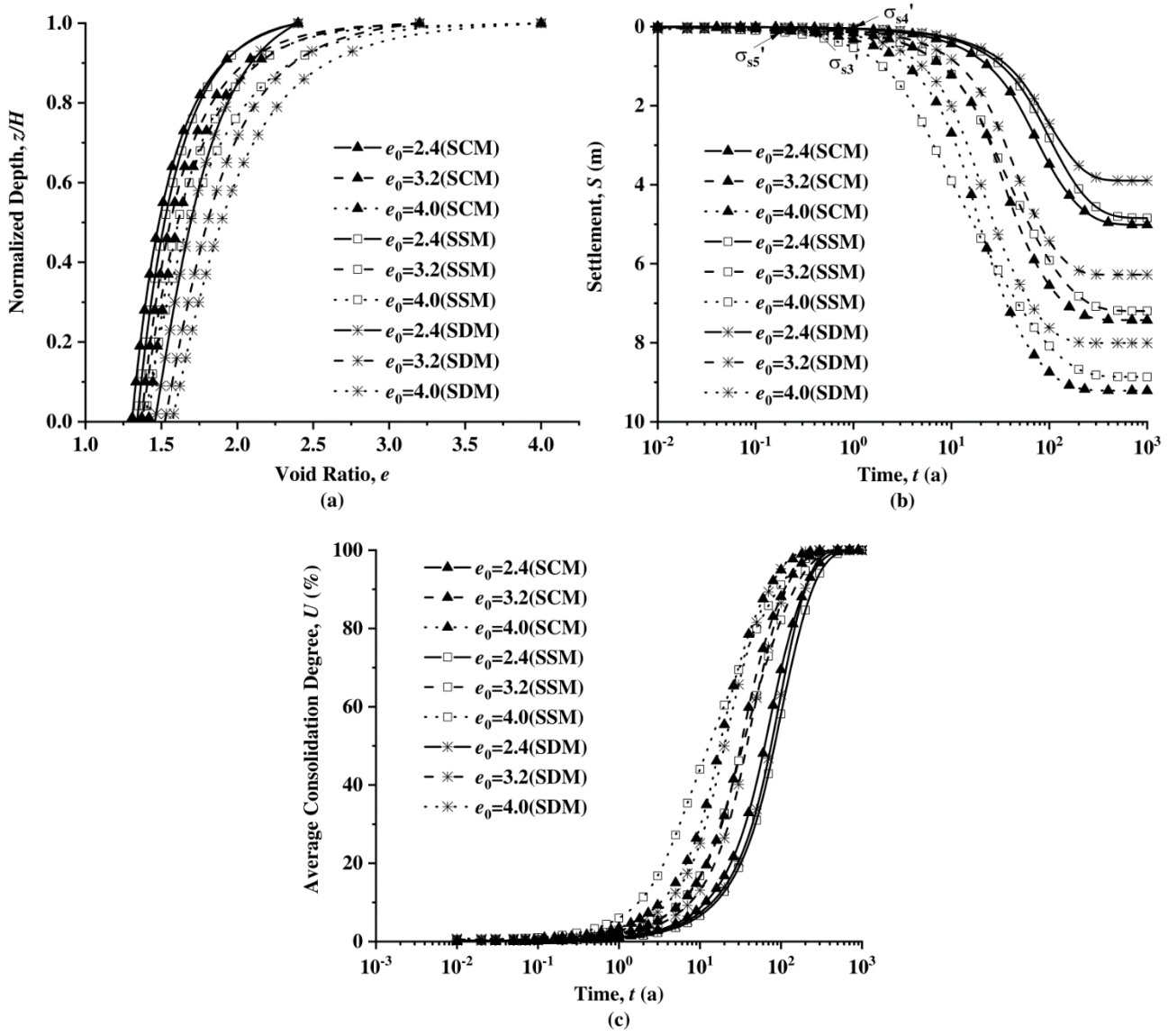

628

629

630 **Fig. 6.** Consolidation behavior of dredged sludge for different initial void ratios: (a) Final void ratio

631 distribution; (b) Settlement; (c) Average consolidation degree

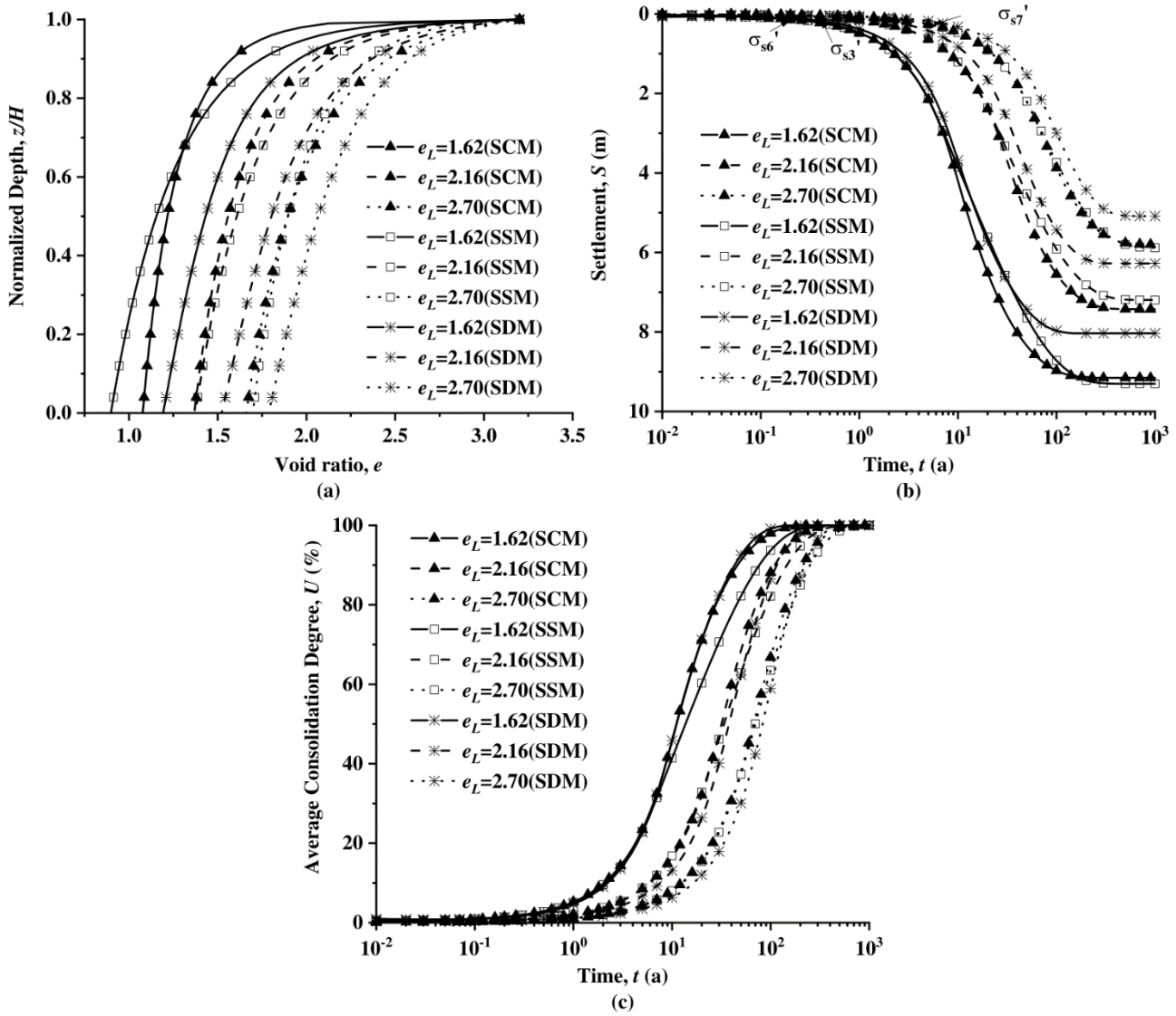

632

633

634 **Fig. 7.** Consolidation behavior of dredged sludge for different void ratios at liquid limit: (a) Final void

635 ratio distribution; (b) Settlement; (c) Average consolidation degree

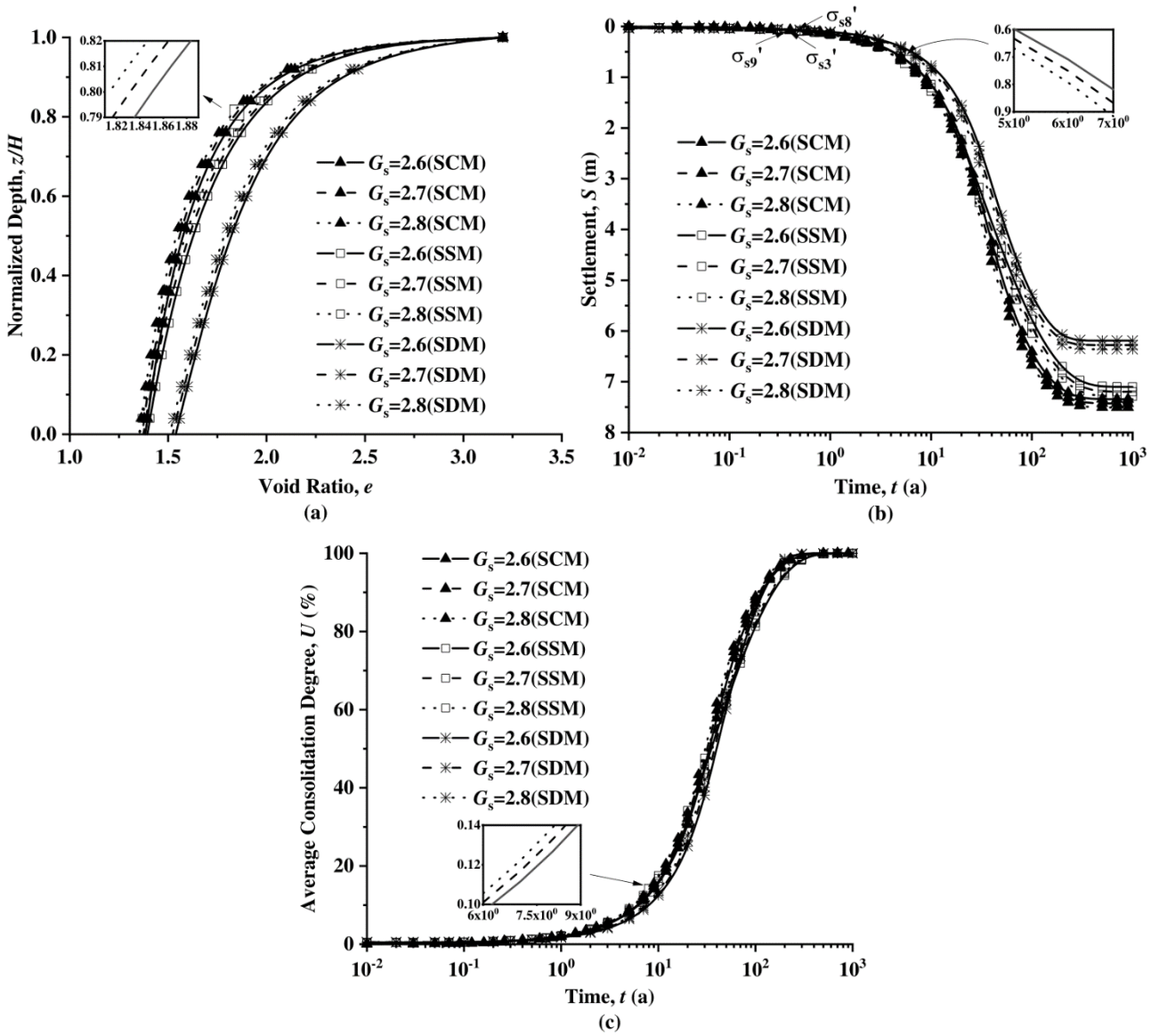

636

637

638 **Fig. 8.** Consolidation behavior of dredged sludge for different specific gravity of soil particles: (a)

639 Final void ratio distribution; (b) Settlement; (c) Average consolidation degree

640